encit 2020

ABCM Associação Brasileira de Engenharia e Ciências Mecânicas

18th Brazilian Congress of Thermal Sciences and Engineering
November 16-20, 2020(Online)

ENC-2020-0631
DIRECT AND INDIRECT OPTIMIZATION OF CFD EXPERIMENTS IN MICROFLUIDICS: A STUDY OF CASE

Pedro Vitor Pantoja de Almeida
Marcos de Souza
pvpalmeida2@uem.br
msouza2@uem.br

Alexandre Marconi de Souza da Costa
Universidade Estadual de Maringá – UEM - Av. Colombo,5790 – Zona 7, 87029900,Maringá, PR, Brasil.
amscosta@uem.br

Abstract. Optimization methods using CFD experiments has becoming an important tool in engineering design in recent years. Besides substantial cost savings over physical experiments, a well verified and validated CFD model can be used as a guidance for new physical experiments as well. Optimization algorithms can be directly applied for the CFD runs, yielding a set of iterative design points towards the maximization (or minimization) of one or more objectives. In contraposition when the Indirect Optimization approach is employed, the optimization algorithms are applied to a surrogate model (response surface). In this work, it is explored both approaches for a microfluidics static mixer. The set of characteristics of both approaches is discussed.

Keywords: *Obstacles in microchannel, Microfluidic, Optimization Algorithms, Lab-0n-a-Chip, Direct and Indirect Optimization.*

1. INTRODUCTION

Many physical phenomena are onerous or even inaccessible to study by traditional experimental methods. As computing capability has expanded, it has become viable to tackle some of these phenomena by computer code modeling. In such cases, the code can rule as a surrogate for the physical phenomena (Kleijnen, 2015). As in a physical experiment, one can modify the inputs to the code and monitor how the output is changed. Such procedure are labeled computer experiments and are turning into progressively suitable replacement for and complement to physical experiments(Sacks et al., 1989; Welch et al., 1992; Santner et al., 2003). Just to name a few science fieds benefited from this approach: computational fluid dynamics (CFD), computational solid mechanics (CSM), electromagnetics, climate modeling (Roache, 2012).

Originally developed for physical experiments, Design Of Experiments (DOE), is a systematic way of changing process input factors to quantify a cause-effect relationship by an adequate way of choosing design points. There are a wide range of DOE methods available in engineering literature (Funkenbusch, 2004; Wheeler, 2009; Montgomery, 2013; Antony, 2013). A common characteristic of all, it is try to locate sampling points such that the space of random input parameters is explored in the most efficient way, or they try to obtain the required information with a minimum of sampling points.

From a numerical computation point of view, DOE consists on sampling different input points and performing the numerical experiment (CFD simulations) for generating the outputs (CFD results).

Following the generated data from the DOE method the next step can be grouped in a class of procedures named as Response Surface Methods (RS).Quite broad field covered by regression analysis in statistics, RS provides a continuous function variation of the output quantities with respect to the input parameters, i.e. , the generated response surface can be seen as a well defined curve fit procedure through the design points (Wang et al., 2001; Kutner, et al., 2004; Forrester et. al., 2008; Myers et al., 2016).

Commonly targeted as the final step in numerical experiments, it is the finding of the optimal design point. The optimization problem formulation starts with the definition of the single (goal) or multiple objective functions (goals) in terms of the output quantities. In addition, the optimization domain constraints, i.e., the ranges of values for input and response parameters; and weighted goals in terms of their importance needs to be specified (Nocedal and Wright, 2006; Thevenin and Janiga, 2008; Rao, 2009; Salem et al., 2017). By its turn, optimization techniques applied to CFD experiments comprises a large field on their own. Applications ranges from Aerodynamics (Bhatia et al. 2014; Aelai, et. al 2019); Heat Transfer (Salviano et. al, 2015; Sarayia et. al 2019), Cooling Towers (Klimanek et al, 2011), Power

Plants (Kapitler et al., 2012), Indoor Ventilation (Mukhtar et al., 2018), Turbine Design(Jung et al., 2019), Solar Energy(Marais et al., 2015; Moghimi et al., 2017) and Urban Pollution(Craig, et al., 2001).

The set of optimization methods directly applied for the CFD experiments (runs) can be labeled as Direct Optimization, whereas when the optimization is applied to the RS results can be labeled as Indirect Optimization. Fig. 1 depicts the workflow associated to these two types of optimization.

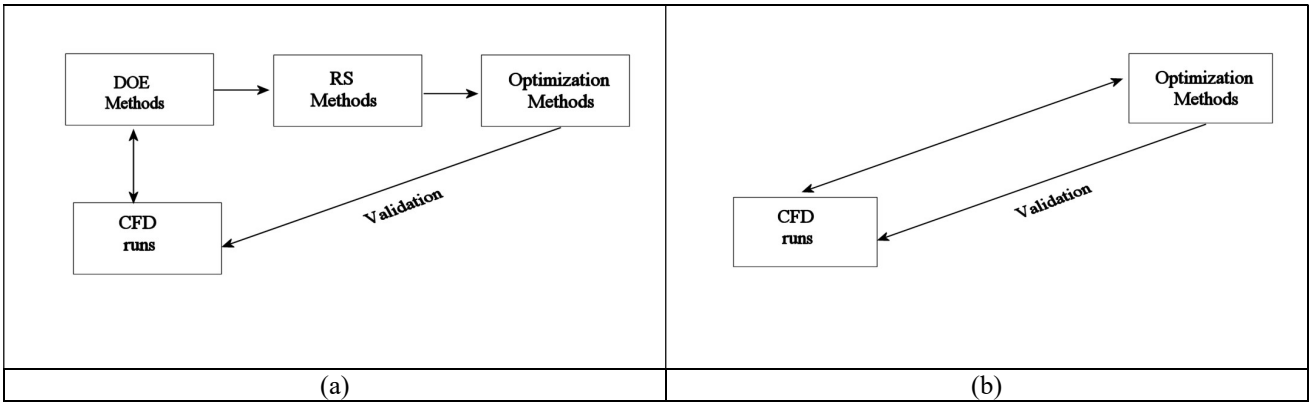

Figure 1. Schemes for indirect (a) and direct (b) optimization.

The workflow of the Direct (Figure b) and Indirect (Figure a) Optimization procedure for CFD numerical experiments is presented in Fig. 1. According to figure 1(b) the Indirect optimization is developed in a three step procedure: the design of experiments (DOE), response surface (RS) generation and Optimization algorithms. In the two step procedure for the Direct optimization, the Optimization algorithms are used in conjunction with the CFD runs.

This paper explores the Direct and Indirect workflow discussed previously for the optimization problem of a microfluidics static mixer. Microfluidics static mixers are miniaturized devices with dimensions ranging from micron to nanometers scales and several applications (Seiffert and Thiele, 2019). With fluid velocities in the laminar regime, providing adequate mixing between different streams in the available channels space is a very important objective.

2. MATERIALS AND METHODOLOGY

The microfluidic mixer model from Almeida, et. al. (2019) is similar to be evaluated numerically in this article is shown in Figure 2.

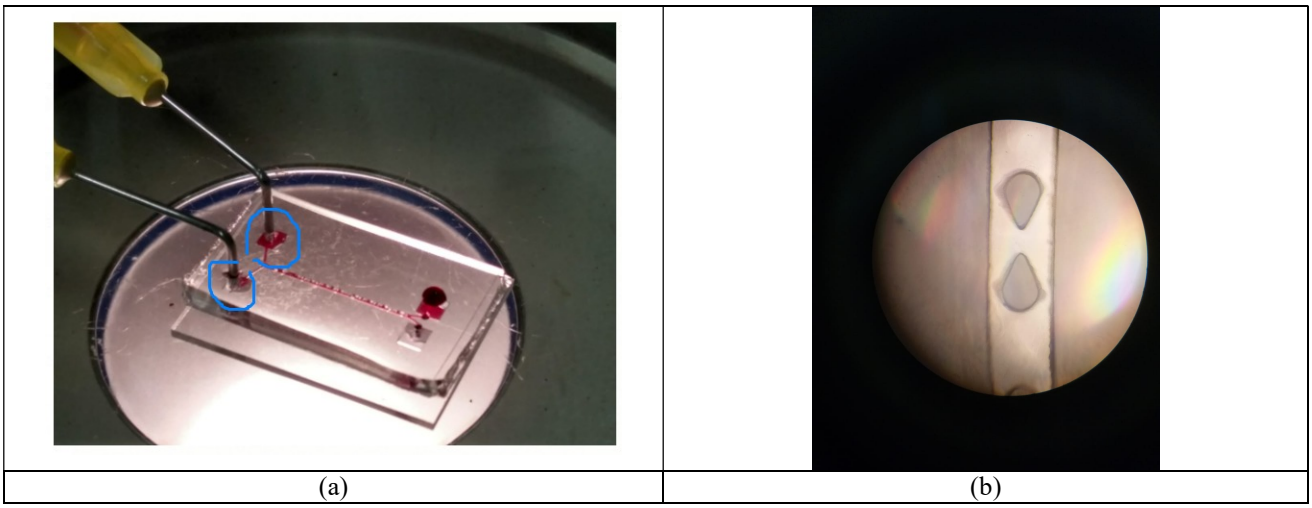

Figure 2. Microfluidic static mixer (a) on chip assembly (b) channel detail.

A schematic drawing of the proposed microfluidic mixer geometry is shown in Figure 3.

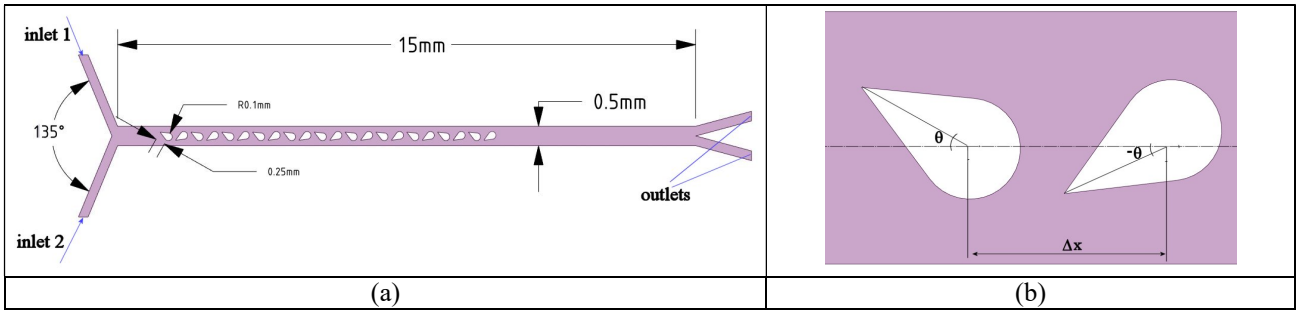

Figure 3. Microfluidic mixer geometry and obstacle detail.

Figure 3(a) presents the plain view of the double Y channel flow with 0.2 mm depth and 22 obstacles. The entrance of the two fluids (pure water and blue methylene aqueous solution at c_o = 10 μg/ml) to be mixed are depicted in the figure. Those inlets corresponds to the two blue sketches draw in Fig 2(a). The range of inlet velocities v_{inlet} were from 0.002 to 0.02 m/s, corresponding to the practical volumetric ranges of our experimental syringe pump device.

Figure 3(b) details the geometric parameters of the inserted obstacles. The obstacles are the junction of circle of radius 0.1 mm and an equilateral triangle with side of 0.25 mm. The alternating angle θ varies from 0 to -90º, and the obstacle horizontal spacing Δx from 0.4 to 0.6 mm.

The CFD experiments were conducted with the ANSYS Fluent 16.0 package. The list of settings were : 3D laminar flow; isothermal; species transport; pressure based solver; steady; no gravity effects; SIMPLE algorithm for pressure velocity coupling; gradient calculation using the least squares cell based; spatial discretization : second order for pressure, second order upwind for momentum and blue methylene specie transport; density by volume-weighted-mixing-law; and constant dilute approximation for the mass diffusivity ($D = 8.3\ 10^{-10}$ m^2/s)

To tackle the workflow depicted in Figure 1 the ANSYS DesignXplorer (DX) was used for the optimization.

For the optimization, the CFD runs were performed for the two independent parameters: θ and v_{inlet} . The output parameter to be maximized and evaluated after each run was the uniformity index γ_a for the blue methylene concentration in a plane located at 14.9 mm from the convergent section, and defined by:

$$\gamma_a = 1 - \frac{\sum_{i=1}^{n}\left(\left|\phi_i - \bar{\phi}_a\right| A_i\right)}{2\left|\bar{\phi}_a\right|\sum_{i=1}^{n} A_i} \quad \text{, where } \bar{\phi}_a = \frac{\sum_{i=1}^{n}\left(\phi_i A_i\right)}{\sum_{i=1}^{n} A_i} \tag{1}$$

In the previous equation i is the facet index of a surface with n facets, ϕ_i and A_i is the blue metilene concentration and area for the ith facet. $\bar{\phi}_a$ is the average valor of the blue metilene concentration over the surface. A highest uniformity is indicated by γ_a close to one.

Table 1 summarizes the set of methods available in DX for indirect and direct optimization. In generating the sampling input parameters for the CFD runs, three well known methods are available: Optimal Space-Filling (OSF), Central Composite Design (CCD) and Box-Behnken Design (BBD) (c.f., Montgomery, 2013). For generating the response surface, three options are also available: Genetic Aggregation (GA) (Holland, 1992; Gen and Cheng, 2000; Haupt and Haupt, 2004; Sivanandam and Deepa, 2008), Polynomial 2nd order (POLY) and Kriging (Myers et al, 2016). Finally, for acquiring the optimal value for the uniformity index in the proposed ranges for θ and v_{inlet}, the following methods are available: Screening (Hammersley and Handscomb, 1964), Nonlinear Programming by Quadratic Lagrangian (NLPQL) from Schittkowski (1986), and from Murata and Ishibuchi (1995) the Multi-Objective Genetic Algorithm (MOGA). For the direct optimization method the Adaptive Single Objective (Rao, 2009) is also available.

Table 1. Methodological options for Indirect and Direct Optimization

	Indirect Optimization	Direct Optimization
DOE methods	Optimal Space-Filling (OSF) Central Composite Design (CCD) Box-Behnken Design (BBD)	none
RS	Genetic Aggregation(GA) Polynomial 2nd order(POLY) Kriging	none
Optimization methods	Screening	Adaptive Single Objective

	Nonlinear Programming by Quadratic Lagrangian(NLPQL) Multi-Objective Genetic Algorithm(MOGA)	Screening Nonlinear Programming by Quadratic Lagrangian(NLPQL) Multi-Objective Genetic Algorithm(MOGA)

3. RESULTS AND DISCUSSION

In Figure 4 is presented the correlation matrix constructed to determine the level of correlation between the complete set of inputs and the output variable. It was generated by using Spearman´s rank correlation(Kutner et al., 2004) whereby 80 samples(CFD runs). This type of correlation detects a monotonic relationship between two variables, being less restrictive than a linear relationship. The 80 samples were generated by using the Latin Hypercube sampling, i.e., input points were randomly placed, but care is taken to ensure that no two points share input parameters of the same value.

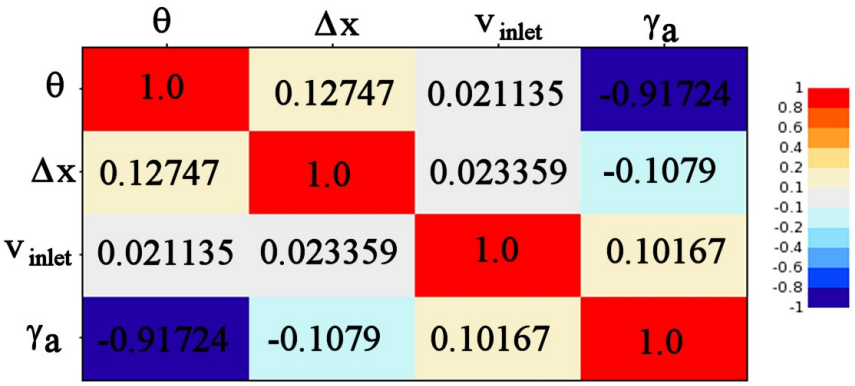

Figure 4. Spearman´s correlation matrix

Analysis of Fig. 4 points to the rotation angle being the most influential parameter in the mixing index with the correlation value –0.91724. The second most influential parameter in the mixing index is the obstacle spacing with a correlation value of –0.1079. The negative sign in both correlation values indicates that when the first parameter increases (angle or obstacle spacing), the second parameter (mixing index) decreases. The positive value correlation (0.10167) indicates an increasing mixing index with an increasing inlet velocity. Based on correlation matrix values, it was chosen one geometric input parameter (angle) and one operational parameter (inlet velocity) for the subsequent direct and indirect optimization studies.

Table 2 and Table 3 presents the results for direct optimization for the Adaptive Single-Objective method, it was found 3 candidates in a maximum of 33 evaluations and 20 domain reductions. The number of initial samples is 8.

Table 2. Direct Optimization Results (Adaptive Single-Objective)

Inputs	Candidate Point 1	Candidate Point 2	Candidate Point 3
Rotation	-80.208	-57.886	-72.288
Velocity inlet	0.016386	0.014198	0.01175681
Output			
Uniformity Index	0.99938	0.98681	0.98477

Analysis of Table 2, indicates there is 2 % in the maxima output values predicted for the 3 candidates points. For the velocity inlet the difference is 30 % and for the rotation angle 28 %. The results indicate the method predicts the maxima of the mixing for greater (close to vertical) rotation angles.

The indirect optimization workflow results are presented the next paragraphs.

First, Figure 5 presents the distribution of the inclination angle θ and the inlet velocity v_{inlet} generated for the deferent DOE methods. From Figure 5, the BBD method places the CFD run points (triangles) in the outermost

boundary of the domain. Whereas for CCD is sampled an innermost square pattern with a central point in the domain (diamonds). The OSF method tries to spread with the equal distance the points (squares) in the domain.

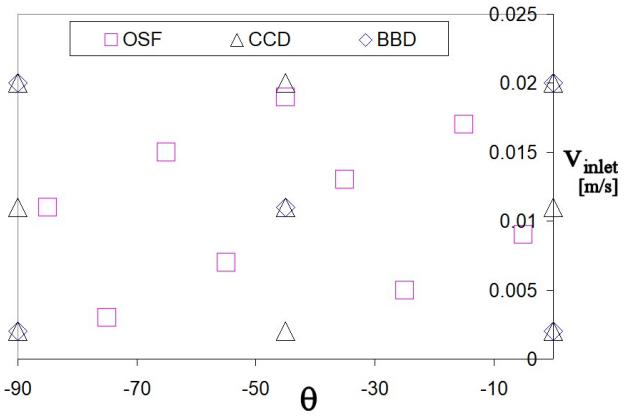

Figure 5. Distribution of input parameters in the design space from the different DOE methods.

The next step performed in the indirect optimization consisted of the generation of the response surfaces, i.e., surfaces that show the variation of the output parameter concerning one or two input parameters at a time.

Two different response surfaces were generated using the methods depicted in table 1: Genetic Aggregation (GA) and Kriging. Eighty refinement points were appended for the initial DOE design point set to improve the quality of the response surface. Figures 6 depicted a typical plot of a generated response surface, along with the design points (DOE points plus refinement points). It must be noticed the good coincidence through the majority of the design points (greyed squares). Due to the refinement strategy, this was observed for all the two RS methods chosen.

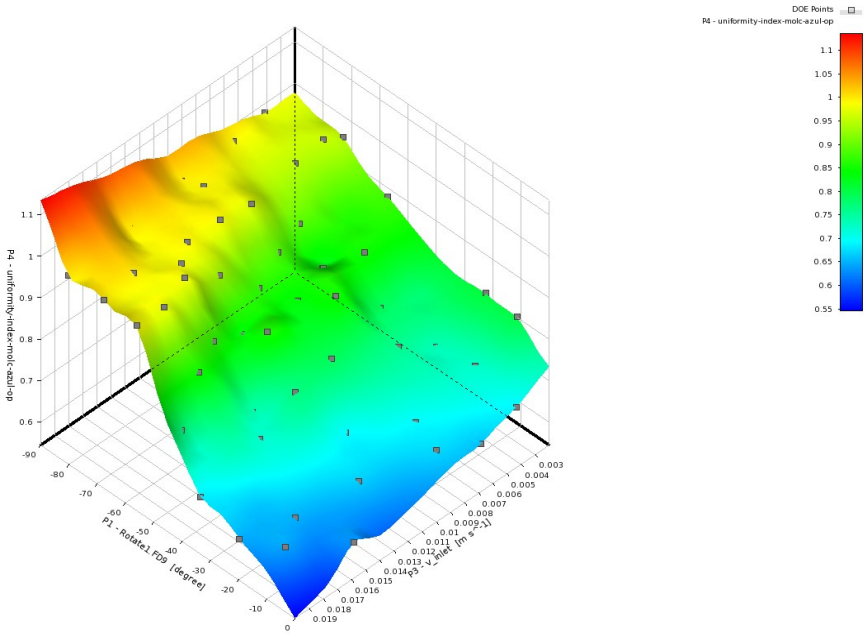

Figure 6. Typical response surface and design points (greyed squares).

The degree of agreement with RS predicted and observed data, termed here as a goodness of fit, is also shown in Figure 7. The match between the response surface predicted and the CFD runs were exact for the design points (square dots). For the verification points (circle dots), i.e., points generated by CFD runs but not used for the response surface construction the match is approximate.

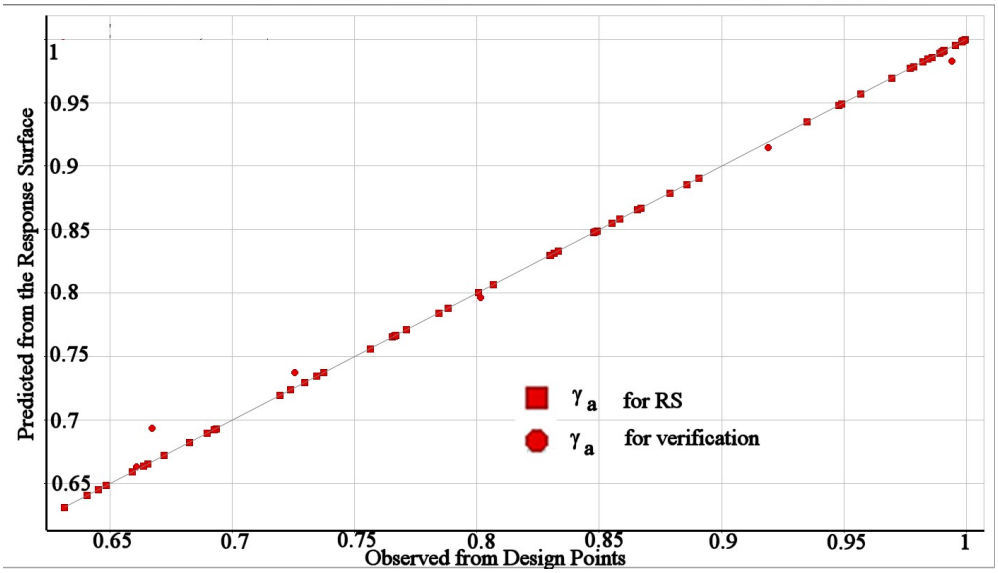

Figure 7. Typical goodness of fit.

The results for the indirect optimization for different response surface and optimization methods are summarised in Table 4 , Table 5, Table 6. It is also shown, the percentual difference ε is given by:

$$\varepsilon = 100\ \frac{\left(\gamma_{\text{a-CFD}} - \gamma_{\text{a-RS}}\right)}{\gamma_{\text{a-CFD}}} \tag{2}$$

Where $\gamma_{\text{a-CFD}}$ corresponds to the CFD calculated value and $\gamma_{\text{a-RS}}$ corresponds to the response surface value. Bar chart plots of ε are depicted in Figures (4), (5), and (6).

Table 4. OSF DOE

RS/Optimization Methods	Kriging /Screening	Kriging /MOGA	Kriging /NLPQL	GA/ Screening	GA/ MOGA	GA/ NLPQL
Input Parameters						
θ	-76.725	-80.55	-79.935	-83.025	-87.928	-85.39
v_{inlet}	0.016142	0.014599	0.014453	0.014525	0.010528	0.012906
Output Values						
$\gamma_{a\text{-RS}}$	0.99937	0.9996	1.0	0.99995	0.99992	1.0
$\gamma_{a\text{-CFD}}$	0.99973	0.99843	0.99876	0.99848	0.99619	0.99843
ε	0.03601	-0.11718	-0.12415	-0.14722	-0.37443	-0.15725

Table 5 - CCD DOE

RS/Optimization Methods	Kriging /Screening	Kriging /MOGA	Kriging /NLPQL	GA/ Screening	GA/ MOGA	GA/ NLPQL
Input Parameters						
Rotation	-74.205	-69.206	-73.846	-83.925	-68.558	-45.135
Velocity Inlet	0.019236	0.017721	0.011465	0.01565	0.018466	0.010928
Output Values						
$\gamma_{a\text{-RS}}$	0.99998	0.99904	0.99684	0.99998	0.9983	0.89785
$\gamma_{a\text{-CFD}}$	0.99973	0.99678	0.99285	0.99897	0.99861	0.83714
ε	-0.02501	-0.22673	-0.40187	-0.1011	0.031043	-7.25207

Table 6 - BBD DOE

RS/Optimization Methods	Kriging /Screening	Kriging /MOGA	Kriging /NLPQL	GA/ Screening	GA/ MOGA	GA/ NLPQL
Input Parameters						
Rotation	-62.685	-70.198	-82.114	-78.885	-69.462	-45.048
Velocity Inlet	0.0192	0.017888	0.011378	0.017618	0.016632	0.01084
Output Values						
$\gamma_{a\text{-}RS}$	0.99995	0.99983	1.0	0.99998	0.99994	0.90577
$\gamma_{a\text{-}CFD}$	0.99113	0.9986	0.99568	0.81931	0.99679	0.83409
ε	-0.88989	-0.12317	-0.43387	-22.015	-0.31601	-8.5938

From Table 4, analysis of the optimization results derived from the OSF DOE and Kriging indicates that there is a 5 % difference for the θ value corresponding to the maxima outputs. Whereas, there is an 11 % difference in the values of the v_{inlet} corresponding to the maxima.

By its turn, results from the optimization of GA generated response surface show that there is a difference in the input parameters pointing to the maxima of 6% (θ) and 28 % (v_{inlet}), respectively. Also from Table 4, for the maxima output values(best mixing), the differences is 0.027 % for the Kriging and 0.008 % for the GA.

From Table 5, analysis of the optimization results derived from the CCD DOE and Kriging indicates that there is a 7 % difference for the θ value corresponding to the maxima outputs. Whereas, there is a 41 % difference in the values of the v_{inlet} corresponding to the maxima. By its turn, for the GA response surface, there is a difference in the input parameters pointing to the maxima of 46% (θ) and 41% (v_{inlet}), respectively. For the CCD DOE sampling space, for the maxima output values the differences 0.009 % for the Kriging and 10 % for the GA response surface.

From Table 6, analysis of the optimization results derived from the BBD DOE and Kriging indicates that there is a 34 % difference for the θ value corresponding to the maxima. Whereas, there is a 41 % difference in the values of the v_{inlet} corresponding to the maxima of the output values . By its turn, for the GA response surface, there is a difference in the input parameters pointing to the maxima of 43% (θ) and 39% (v_{inlet}), respectively. For the BBD DOE sampling space, for the maxima output values the differences 0.0017 % for the Kriging and 9 % for the GA.

The bar charts from Figures 4, 5, and 6, illustrate quantitatively the degree of agreement between the predicted maxima from the response surface fitting and the CFD runs.

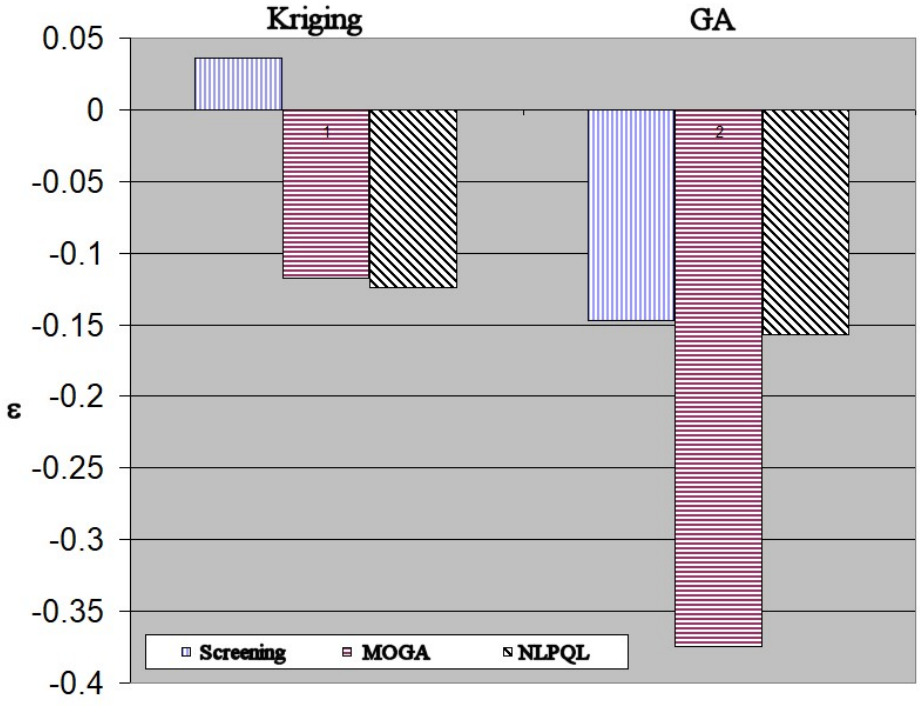

Figure 4. DOE method OSF : Percentual difference for different RS and Optimization methods.

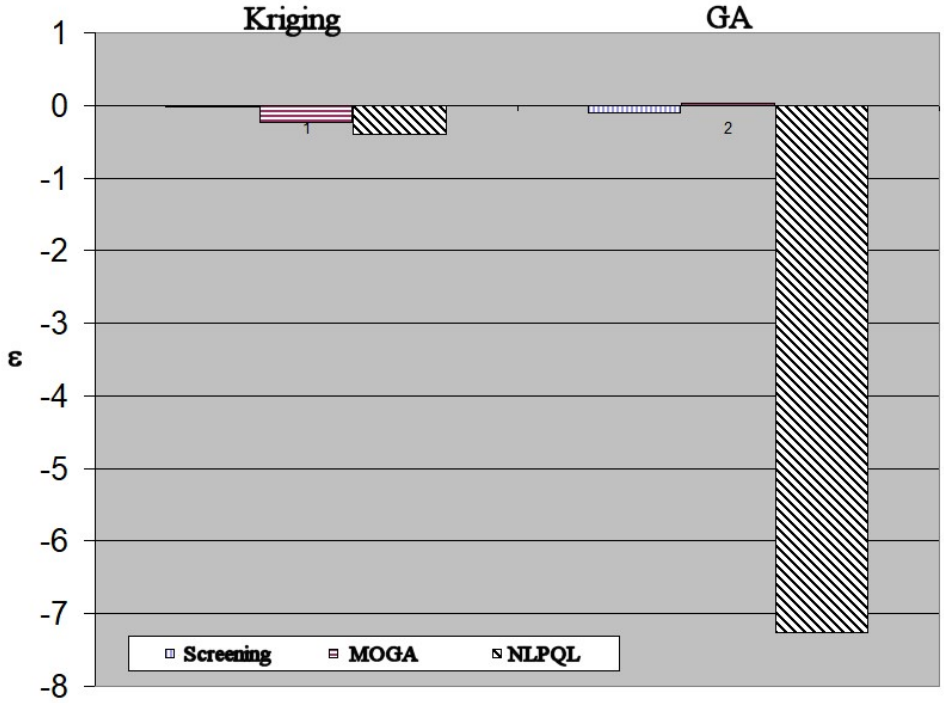

Figure 5. DOE method CCD : Percentual difference for different RS and Optimization methods.

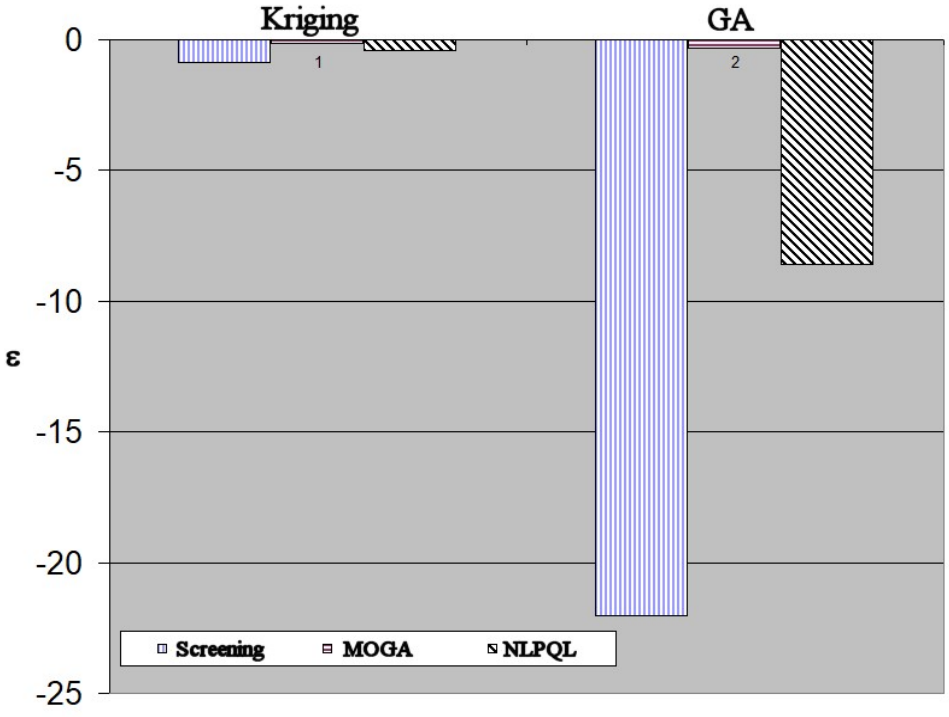

Figure 6. DOE method BBD : Percentual difference for different RS and Optimization methods.

Analysis of the bar chart from Figure 4 shows that for OSF sampling, and the two different RS methods (Kriging, GA) the maximum difference of the optimal value of mixing index from the CFD results are below –0.4 %. The lowest difference, around 0.03 % was obtained using the Screening optimization method. In short, for the OSF sampling scenarios, all three optimization methods resulted in good agreement with the CFD verification results.

Analysis of the bar chart from Figure 5 shows that for CCD sampling, and the two different RS methods (Kriging, GA) the maximum difference of the optimal value of mixing index from the CFD results are below –0.4 % for Kriging

and around –7 % for NLPQL. Again, the lowest value, around -0.025 % was obtained using the Screening optimization method.

Analysis of the bar chart from Figure 6 shows that for BBD sampling, and the two different RS methods (Kriging, GA) the maximum difference of the optimal value of mixing index from the CFD results are below –-0.88989 % for Kriging and below –22 % for GA worst-case scenario (NLPQL). The lowest value, around -0.12 % was obtained using the MOGA optimization method.

A final comparison with the direct methods from Table 1 results, and indirect results of Table 2, Table 3, and Table 4, indicates the best agreement triplet (OSF-Kriging-Screening) with a 0.001 % difference for the output value maxima for the ASO first candidate. For this best triplet the input differs 5 % for the rotation and 1 % for the velocity inlet.
The worst-case agreement in outputs for all direct optimization candidate points and the response surface generated if for the triplet CCD-GA-NLPQL with an 11 % difference for the output value maximum. For this worst agreement, the input differs 56 % for rotation and 50 % for velocity inlet.

4. CONCLUSION

It was depicted the difference in results for the Indirect Optimization methods when using different DOE samplings, Response Surface methods and Optimization Algorithms. A comparison with the Direct Optimization pointed for the best DOE sampling , RS and Optimization Algorithm to be employed. The optimization methods when applied to the generated response surfaces show significant drift in the values of the input values for maxima output values. By its turn, the maxima values the distinction is minor.

For the microfluidics static mixer optimization studied, the degree of agreement of the maxima values predicted for the best DOE-RS-Optimization algorithm triplet is excellent and it was achieved for the triple OSF-Kriging-Screening. As the purpose of generating RS is to speed up evaluations and optimization, the finding of the best triplet is a worthwhile task.

The comparison between maxima values (input + output) points for different methods along with the degree of agreement with the verified CFD runs provides a guideline for the best pair RS/Optimization method be chosen. This pair search can also be applied to other practical optimization studies in engineering practice.

5. REFERENCES

Acar, E. *Various Approaches for Constructing an Ensemble of Metamodels Using Local Measures, Structural and Multidisciplinary Optimization*, v. 42, n.6. p 879-896, 2010.

Aelai, M.; KARIMIAM, S.; OMMI, F. Sensitivity Analysis and Optimization of Delta Wing Design Parameters using CFD-Based Response Surface Method, *Journal of Applied Fluid Mechanics*, v.12, n6, pp 1885-1903, 2019.

Almeida,P.V.P.;Souza,M.;Costa,A.M.S.Análise Numérica e experimental aplicando CFD no escoamento sobre obstáculos em Microcanais.In: XI EPCC - Encontro Internacional de Produção Científica, 2019, Maringa. Anais Eletrônico do XI EPCC - Encontro Internacional de Produção Científica. Recife- PE:: Even3, 2019.

Antony, J. *Design of Experiments for Engineers and Scientists*, Elsevier, 2013.

Bhatia,V.; Karthikeyan, R.; Ram, R. K. G.; Cooper, Y. N. Design Optimisation and Analysis of a Quadrotor Arm using Finite Element Method, *Applied Mechanics and Materials*, v. 664, p. 371-375, 2014.

Craig, K. J.; Kock, D. J.; Snyaman, J. A. Minimising the effect of automotive pollution in a urban geometry using mathematical optimization, *Atmospheric Environment*, 35, p. 579-587, 2001.

Forrester, A. I. J.; Sobester, A.; Keane, A. J. *Engineering Design via Surrogate Modelling*, Wiley, 2008.

Funkenbusch, P. D. *Practical Guide to Designed Experiments – A Unified Modular Approach*, CRC Press, 2004.

Gary,W.; Dong, Z.; Aitchison, P. Adaptive Response Surface Method -- A Global Optimization Scheme for Computation-intensive Design Problems, *Journal of Engineering Optimization*, Vol. 33, pp.707-734, 2001.

Gen, M., Cheng, R. *Genetic Algorithms and Engineering Optimization*, Wiley, 2000.

Hammersley, J. M.; Handscomb, D.C. *Monte Carlo Methods*, Wiley, New York , 1964.

Haupt , R. L.; Haupt, S. E.; *Practical Genetic Algorithms*, Second Edition, Wiley, 2004.

Holland, J. H. *Adaptation in Natural and Artificial Systems*, MIT Press, 1992.

Jung, H.; Kanemoto, T.,; Liu, P.; Murakami, T. A Numerical Study on Performance Improvement of Counter-Rotating Type Tidal Stream Power Unit, IOP *Conf Series: Earth and Environmental Science*, 240, 2019.

Kapitler, M.; Samec, N.; Kokalj, F.; Operation of Waste to Energy Plant Optimisations by Using Design Exploration, *Advances in Production Engineering & Management*, 7, 2, 101-112, 2012.

Kleijnen, J. P. C. *Design and Analysis of Simulation Expe*riments, Springer, 2015.

Klimanek, A.; Musiol, T.; Stechman, A. Optimization of Guide Vane Positions in Bended Inflow of Mechanical Draft Wet-Cooling Tower, *Archives of Thermodynamics*, v.32, n3, p.263-272, 2011.

Marais, M. D., Craig, K. J., Meyer, J. P., 2015, Computational flow Optimization of Heliostat Aspect Ratio for Wind Direction and Elevation Angle, *Energy Procedia*, v. 69, p.148-157.

Moghimi, M. A., Craig, K. J., Meyer, J.P., 2017, Simulation-based Optimisation of a Linear Fresnel Collector Mirror Field and Receiver for Optical, Thermal and Economic Performance, *Solar Energy*, v. 153, p. 655-678.

Montgomery, D. C., *Design and Analysis of Experiments*, Wiley, 2013.

Mukhtar, A, NG K.C.,Yusoff, M.Z., Design Optimization for Ventilation Shafts of Naturally-Ventilated Underground Shelters for Improvement of Ventilation Rate and Thermal Comfort, *Renewable Energy*, doi: 10.1016/j.renene.2017.08.051, 2017.

Mukhtar, A. , Yusoff, M. Z., NG, K. C., Nasir, M. F. M., 2018, Application of Box-Behnken Design with Response Surface to Optimize Ventilation System in Underground Shelter, *Journal of Advanced Research in Fluid Mechanics and Thermal Sciences*, v.52, n.12, p.161-173.

Murata,T., Ishibuchi, H., MOGA: Multi-objective Genetic Algorithms, *Proc. of 1995 IEEE International Conference on Evolutionary Computation*, pp. 289-294, Perth, Australia, November 1995.

Nocedal, J.; Wrigth, S. *Numerical Optimization*, Springer, 2006.

Rao, S. S*., Engineering Optimization – Theory and Practice*. Wiley, 2009.

Roache, P. J., *A Defense of Computational Physics*, 2012, Hermosa Publishers.

Sacks, J.; Welch, W. J.; Mitchell, T. J.; Wynn, H. P., Design and Analysis of Computer Experiments, *Statistical Science*, v. 4, n.4, 409-435, 1989.

Salem, M. B., Roustant, O., Gamboa, F., Tomaso, L. Universal Prediction Distribution for Surrogate Models, SIAM *Journal Uncertainty Quantification*, v.5, p. 1086-1109, 2017.

Salviano, L. O., Dezan, D. J., Yanagihara, J. I.Optimization of winglet-type vortex generator positions and angles in plate-fin compact heat exchanger: Response Surface Methodology and Direct Optimization, *International Journal of Heat and Mass Transfer*, 82, p.373-387, 2015.

Santer, T. J., Williams, B. J., Notz, W. I., *The Design and Analysis of Computer Experim*ents, Springer, 285p., 2003.

Saraya, A.; Chandramohan, V. P.; Balasubramanian, K. Optimization for Horizontal Rectangular Fin Heat Sink: a CFD with Response Surface Analysis and Parametric Study, *Journal Institute Engineers India C*, 2019.

Schittkowski, K. NLPQL: A fortran subroutine solving constrained nonlinear programming problems. *Annals of Operation Research,* 5(2), 485-500, 1986.

Seiffert, S., Thiele, J., *Microfluidics: Theory and Practice for Beginners*, Walter de Gruyter GmBH & Co KG, 295p, 2019.

Sivanandam,S.N., Deepa, S.N., *Introduction to Genetic Algorit*hms, Springer, 2008.

Thevenin, D., Janiga, G., *Optimization and Computational Fluid Dynamics*, Springer, 2008.

Viana, F. A. C., Haftka, R. T., Steffen, V., Multiple Surrogates : How Cross-Validation Errors Can Help Us to Obtain the Best Predictor, *Structural and Multidisciplinary Optimization*, v.39, n.4, p. 439-457., 2009.

Welch, W. J., Buck, R. J. Sacks, J. Wynn, H. P., Mitchell, T. J., Morris, M. D. *Screening, Predicting, and Computer Experiments, Technometrics*, v. 34, n.1, 15-25, 1992.

Wheeler, A. J., Ganji, A. R., *Introduction to Engineering Experimentation*, Pearson, 2009.

6. RESPONSIBILITY NOTICE

The author(s) is (are) the only responsible for the printed material included in this paper.